A Fourth-Order Partial Differential Equations Method Of Noise Removal

Xilin Liu
Department of Mathematics
East China Institute of Technology
Nanchang, Jiangxi, China. 330013

Zhengwei Ying
School of Science
East China Institute of Technology
Nanchang, Jiangxi, China. 330013

Shufang Qiu
School of Science
East China Institute of Technology
Fuzhou, Jiangxi, China. 330013

***Abstract*—In this paper, we introduce a new method for image denoising based on a fourth-order partial differential equation (PDE) model and a mean curvature diffusion (MCD) model. The fourth-order PDE model can cause less blocky effect and preserve edges in image denoising. But it loses too much texture in the restored image. The mean curvature diffusion model can keep texture while quickly removing noise. So we introduce the mean curvature diffusion into the PDE-based noise removal algorithm. Finally, Numerical experiments are done by our proposed model. We also compared our method with the fourth-order PDE model and the mean curvature diffusion model. Numerical examples show that the proposed model can preserve fine structure and keep texture well while quickly removing image's noise.**

I. Introduction

The presence of noise in image is unavoidable because of the environment during image acquisition and the imaging system during image transmission. So, noise removal is one of the important parts in image processing. The main purpose of image denoising is to restore or reconstruct a true image u from a degraded image f. Suppose that there is a 2D image function f defined on Ω, where $\Omega \subset \mathbb{R}^2$ is a bounded and open domain, the denoising procedure is to extract u from f. Numerous partial differential equations (see [5, 10, 11, 12,] and [8, 9]) have been proposed to remove noise. However, these conventional PDE-based models may lose interesting fine structures during the denoising. As a consequence, many other PDE-based denoising models have been proposed, and have much success in preserving structures while removing noise. Besides, geometry-driven also has a wide range of applications in image denoising.

A class of fourth order PDE model for denoising has been derived in [1], the main model is as follows:

$$E(u) = \int_{\Omega} f\left(\|\triangle u\|\right) dxdy \tag{1}$$

Where the function $f(\cdot) \geqslant 0$ and is an increasing function. It can keep edges better while removing noise. However, speckles are more visible in images processed by (1). Other fourth-order PDE models, see in [5-7], are proposed. These new models may preserve fine structures better. However, more advanced models are yet to be developed.

At the same time, geometry-driven image diffusion [4] has been studied as a useful tool for image restoration. [12] Gives a model for denoising with Gauss Curvature-Driven diffusion. In [2] an inhomogeneous mean curvature diffusion model is introduced. Let $u(x, y)$ denote the image intensity function. The scalar equation of the mean curvature diffusion in [2, 3, 4] is obtained as follows:

$$\frac{\partial u}{\partial t} = \frac{\partial}{\partial x}\left(\frac{u_x}{\sqrt{u_x^2 + u_y^2 + 1}}\right) + \frac{\partial}{\partial y}\left(\frac{u_y}{\sqrt{u_x^2 + u_y^2 + 1}}\right) = H$$

Where

$$H = \frac{u_{xx}\left(1 + u_y^2\right) - 2u_x u_y u_{xy} + u_{yy}\left(1 + u_x^2\right)}{\left(u_x^2 + u_y^2 + 1\right)^{3/2}}$$

is the mean curvature of the image intensity surface $(x, y, u(x, y))$. As we know, this model can remove noise quickly.

In this article, we combine the mean curvature diffusion denoising method (2) with the fourth-order PDE model (1) for noise removal. Then, an improved model is proposed for image denoising. The rest of this paper is organized as follows. In Section II, we introduce the new noise-removal model and its implement algorithm. In Section III, we present some numerical experiments, along with comparison among the fourth-order PDE model of [1], MCD model of [2] and our new model. Finally, section IV gives some conclusion.

II. Improved model for noise removal

Firstly, we propose the improved model for noise removal as follows:

$$\frac{\partial u}{\partial t} = -\lambda\Delta[c\left(|\Delta u|\right)\Delta u] + (1-\lambda)H, \tag{2}$$

with the boundary condition

$$\frac{\partial u}{\partial n} = 0 \quad on\partial\Omega,$$

where

$$c\left(|\Delta u|\right) = \frac{f'\left(|\Delta u|\right)}{|\Delta u|},$$

and $0 \leqslant \lambda \leqslant 1$ is a constant. It is easy to see that equation (2) is the method of [2] if $\lambda = 0$, and equation (2) becomes the method of [1] if $\lambda = 1$. Partial differential equation (3) may be solved numerically using the following iterative approach

$$\frac{u^{(n+1)} - u^{(n)}}{\Delta t} = -\lambda\Delta[c\left(|\Delta u|\right)] + (1-\lambda)H.$$

978-1-4244-9306-7/11/$26.00 ©2011 IEEE

where λ is a constant that may be adjusted for a specific application. We quantize u in the time and the spatial domain as follows:

$$t = n\Delta t, n = 0, 1, 2, \cdots$$
$$x = i\Delta x, i = 1, 2, \cdots, M,$$
$$y = i\Delta y, i = 1, 2, \cdots, N.$$

At the first stage, let's consider the first term on the right of the equation. The Laplace of the intensity function u at pixel (i, j) is as follows:

$$\Delta u_{i,j}^n = \frac{u_{i+1,j}^n + u_{i-1,j}^n + u_{i,j+1}^n + u_{i,j-1}^n - 4u_{i,j}^n}{h^2},$$

for $i = 1, 2, \cdots M$; $j = 1, 2, \cdots, N$, with boundary conditions

$$u_{0j}^n = u_{1j}^n, u_{N+1,j}^n = u_{N,j}^n, u_{i0}^n = u_{i1}^n, u_{i,N+1}^n = u_{iN}^n,$$
$$u_{00} = u_{11}, u_{0,N+1} = u_{1,N},$$
$$u_{M+1,0} = u_{M,1}, u_{M+1,N+1} = u_{M,N}.$$

Let $f(\Delta u) = c(|\Delta u|)\Delta u$, thus $f_{i,j}^n = f\left(\Delta u_{i,j}^n\right)$.

$$\begin{aligned}\Delta\left[c(|\Delta u|)\Delta u\right]_{i,j}^n &= \Delta f_{i,j}^n \\ &= \frac{f_{i+1,j}^n + f_{i-1,j}^n + f_{i,j+1}^n + f_{i,j-1}^n - 4f_{i,j}^n}{h^2}.\end{aligned}$$

At the second stage, we consider the second term on the right of the equation.

$$\begin{aligned}H_{i,j}^n =& \frac{\partial}{\partial x}\left(\frac{u_x}{\sqrt{u_x^2+u_y^2+1}}\right)_{i,j}^n + \frac{\partial}{\partial y}\left(\frac{u_y}{\sqrt{u_x^2+u_y^2+1}}\right)_{i,j}^n \\ =& \left(\sum_{p=i-1}^{i+1}\sum_{q=i-1}^{i+1}\frac{1}{8\left|\nabla g_{p,q}\right|}u_{p,q}^n - \frac{1}{8\left|\nabla g_{p,q}\right|}\right)u_{i,j}^n \\ &- \left(\sum_{p=i-1}^{i+1}\sum_{q=i-1}^{i+1}\frac{1}{8\left|\nabla g_{p,q}\right|} - \frac{1}{8\left|\nabla g_{p,q}\right|}\right)u_{i,j}^n \\ =& u_{i,j}^n + \frac{1}{8|\nabla g_{i-1,j-1}|}u_{i-1,j-1}^n + \frac{1}{8|\nabla g_{i-1,j}|}u_{i-1,j}^n \\ &+ \frac{1}{8|\nabla g_{i-1,j+1}|}u_{i-1,j+1}^n + \frac{1}{8|\nabla g_{i,j-1}|}u_{i,j-1}^n \\ &+ \frac{1}{8|\nabla g_{i,j+1}|}u_{i,j+1}^n + \frac{1}{8|\nabla g_{i+1,j-1}|}u_{i+1,j-1}^n \\ &+ \frac{1}{8|\nabla g_{i+1,j}|}u_{i+1,j}^n + \frac{1}{8|\nabla g_{i+1,j+1}|}u_{i+1,j+1}^n \\ &- \left(\frac{1}{8|\nabla g_{i-1,j-1}|} + \frac{1}{8|\nabla g_{i-1,j}|} + \frac{1}{8|\nabla g_{i-1,j+1}|}\right. \\ &+ \frac{1}{8|\nabla g_{i,j-1}|} + \frac{1}{8|\nabla g_{i,j+1}|} + \frac{1}{8|\nabla g_{i+1,j-1}|} \\ &\left.+ \frac{1}{8|\nabla g_{i+1,j}|} + \frac{1}{8|\nabla g_{i+1,j+1}|}\right)u_{i,j}^n.\end{aligned}$$

Finally, the numerical approximation to the differential equation is given as :

$$u_{i,j}^{n+1} = u_{i,j}^n - \Delta t\lambda\Delta f_{i,j}^n + \Delta t(1-\lambda)H_{i,j}^n.$$

III. Numerical experiments

In this section, we will verify our proposed image denoising model considered in the previous section. We apply our proposed model to the restoration of many images. The signal to noise ratio (SNR) is defined as follows:

$$SNR = \frac{\sum_\Omega (u_{i,j} - \overline{u})^2}{\sum_\Omega (n_{i,j})^2},$$

where $\overline{u}$ is the mean of original image, $u_{i,j}$ is the original image intensity at pixel (i, j), Ω is all of the pixels in an image and $n_{i,j}$ is the noise. The noisy images are obtained by adding Gaussian noise at SNR=5dB in our experiments. To analyze the performance of our model, we compare our model with fourth-order PDE model and MCD model. Then, the restoration quality is measured by the mean squared error (MSE) and the peak signal-to-noise ratio(PSNR),which are defined as :

$$MSE = \frac{1}{MN}\int_\Omega (f-u)^2\, dxdy,$$
$$PSNR = 10 \cdot \log_{10}\left(\frac{\sum_{i,j} 255^2}{\sum_{i,j}(f_{ij} - u_{ij})^2}\right),$$

where f is the original image, u denotes the compared image, and the unit of PSNR is dB.

In our experiments, we take $\Delta t = 0.025$, and the following function [3]

$$c(s) = \frac{1}{1 + (s/k)^2}.$$

We set $k = 3$ for $c(s)$ and $\lambda = 0.25$ according to our experiment results. The processed images of different model after 30 iteration times are show in figure 1 and figure 2 with corresponding MSE and PSNR analysis. We find the denoising effect of our model is the best from table 1 and table 2. Figure 3, figure 4 and figure 5 also give the experiment result. But Figure 3, figure 4, and figure 5 don't give the desired results. The fourth-order PDE model removes noise better than the other two models, when applying to images with less texture in figure 3 and figure 4. Figure 5 shows the MCD model processes noise images with much small texture better than the other two models. We find some conditions of being suitable of the fourth-order PDE model, the MCD model and our model. Our model gives a balance between noise and texture of the noisy image to some images with large texture. At last we give the presence of our proposed model to Bag image with λ from 0 to 1 in figure 6 and table 6.

TABLE I: Comparison of the different methods (Bag image)

Methods	MSE	PSNR
Noisy Bag image	864.8504	75.1864
Fourth-Order PDE model	391.2366	166.2038
MCD model	307.4915	211.4693
Our model	246.7899	263.4832

Figure 1 shows the comparison of the Fourth-Order PDE model, MCD model and our model on Bag image. Figure 1(a)

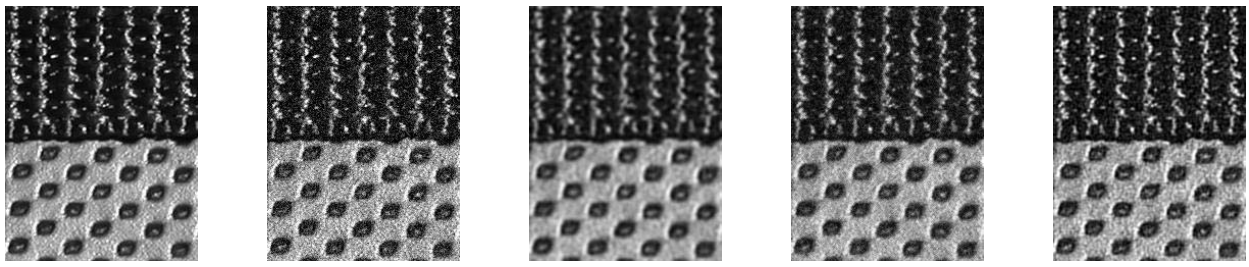

(a) the original image (b) image degraded by 5dB Gaussian noise (c) noise-removal image by the Fourth-Order PDE model (d) noise-removal image by the MCD model (e) noise-removal image by our model

Figure 1. Comparison of the effect on Bag image.

(a) the original image (b) image degraded by 5dB Gaussian noise (c) noise-removal image by the Fourth-Order PDE model (d) noise-removal image by the MCD model (e) noise-removal image by our model

Figure 2. Comparison of the effect on Couple image.

shows the original image. Figure 1(b) shows the noise image degraded by 5dB gaussian noise. Figure 1(c) is the denoised image obtained by Fourth-Order PDE model. Figure 1(d) is the recovered image obtained by MCD model. Figure 1(e) represents our proposed model's result. To get better result, we choose $\lambda = 0.25$ in our model according to the numerical experiment. Table I shows the mean square error (MSE) and the peak signal to noise ratio (PSNR) of figure 1.

TABLE II: Comparison of denoising methods (Couple image)

Methods	MSE	PSNR
Noisy Couple image	469.3859	138.5321
Fourth-Order PDE model	130.7254	497.4166
MCD model	122.7415	529.7719
Our model	117.5431	553.2014

The second example is given to demonstrate the effectiveness of our model. Figure 2 depict the comparison of the models in our paper, which are applied to Couple image. Figure 2(a) is a original image. Figure 2(b) depicts the noise image degraded by 5dB gaussian noise. Figure 2(c) represents the recovered image using fourth-order PDE model and Figure 2(d) is a denoised image using MCD model. Figure 2(e) shows the noise-removal image by our method. Table 2 gives the PSNR and MSE of Figure 2.

Figure 3 shows the comparison of PDE model and MCD model with our model tested on Lady image. Figure 3(a) shows the original Lady image. Figure 3(b) shows the noisy image with 5dB Gaussian noise. Figure 3(c) shows the denoised image of Fourth-Order PDE model. Figure 3(d) shows the result of denoising with MCD model. Figure 3(e) shows the noise-removal image by our model. Table 3 gives the MSE and PSNR comparison of the three models in figure 3.

TABLE III: Comparison of denoising methods (Lady image)

Methods	MSE	PSNR
Noisy Lady image	876.8811	74.1549
Fourth-Order PDE model	101.7920	638.8028
MCD model	231.1957	281.2552
Our model	193.8482	335.4429

TABLE IV: Comparison of denoising methods (Peppers image)

Methods	MSE	PSNR
Noisy Peppers image	716.7752	90.7188
Fourth-Order PDE model	90.7465	716.5565
MCD model	173.0658	375.7241
Our model	150.1378	433.1020

Figure 4 shows the comparison among PDE model, MCD model and our model with application to Peppers image. Figure 4(a) shows the original image. Figure 4(b) shows the noisy image with 5dB Gaussian noise. Figure 4(c) shows the denoised image of Fourth-Order PDE model. Figure 4(d) shows the result of denoising with MCD model. Figure 4(e) shows the noise-removal image by our model. Table 4 gives the MSE and PSNR comparison on Peppers image of the three models.

(a) the original image (b) image degraded by 5dB Gaussian noise (c) noise-removal image by the Fourth-Order PDE model (d) noise-removal image by the MCD model (e) noise-removal image by our model

Figure 3. Comparison of the effect on Lady image.

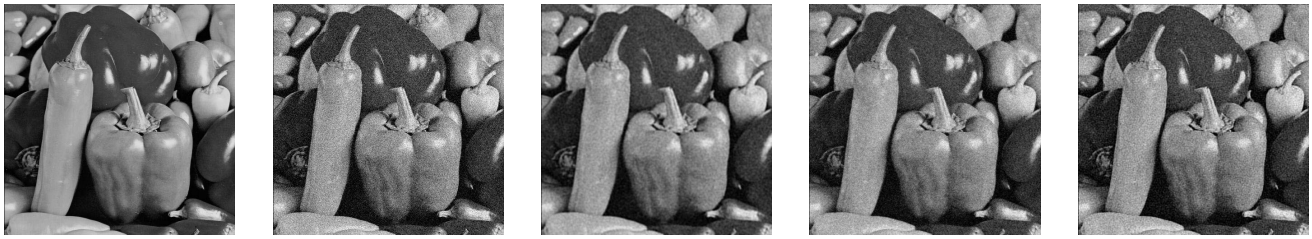

(a) the original image (b) image degraded by 5dB Gaussian noise (c) noise-removal image by the Fourth-Order PDE model (d) noise-removal image by the MCD model (e) noise-removal image by our model

Figure 4. Comparison of the effect on Peppers image.

(a) the original image (b) image degraded by 5dB Gaussian noise (c) noise-removal image by the Fourth-Order PDE model (d) noise-removal image by the MCD model (e) noise-removal image by our model

Figure 5.Comparison of the effect on Woman image.

TABLE V: Comparison of denoising methods (Woman image)

Methods	MSE	PSNR
Noisy Woman image	525.8608	123.6544
Fourth-Order PDE model	260.0381	250.0595
MCD model	178.3912	364.5079
Our model	223.3626	291.1185

Figure 5 shows the denoising effect on Woman image of the Fourth-Order PDE model, MCD model and our model. Figure 5(a) shows the original Woman image. Figure 5(b) shows the noisy Woman image with 5dB Gaussian noise. Figure 5(c) shows the denoised image of Fourth-Order PDE model. Figure 5(d) shows the result of denoising with MCD model. Figure 5(e) shows the noise-removal image by our model. Table 5 gives the MSE and PSNR comparison of the three models in figure 5.

From the first two experiments, we find the MSE of our model is smallest and the PSNR of our model is the largest among the three models. So, it is easy to see from the tables that our model results in better image than the other two models. But from table 3 and table 4, we find the fourth-order model is best while our model is better than the MCD model. However, from table 5 and figure 5, it is not difficult to conclude that the denoising effect on Woman image of MCD model is stronger than the other two models'. We may conclude that each of the three denoising model have its suitable conditions. We find the fourth-order PDE model will lose too much texture and fine structure while denoising, so it is suitable to removal noise on images with less texture, such as the noisy image in figure 3 and figure 4. The MCD model

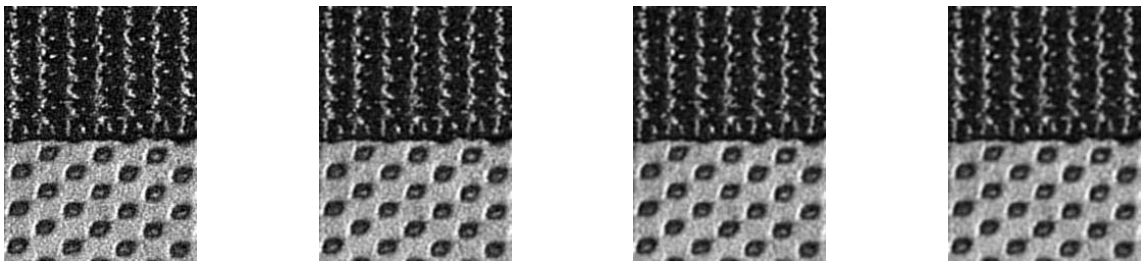

(a) noise removal image with $\lambda = 0.2$ (b) noise removal image with $\lambda = 0.4$ (c) noise removal image with $\lambda = 0.6$ (d) noise removal image with $\lambda = 0.8$

Figure 6. The effect of the noise removal image of our model (on Bag image) with the variation of λ.

may keep texture better than the fourth-order PDE model, but it is not as good as the fourth-order PDE model on the smooth area of the image. So, if the noisy image is smooth, we may choose the fourth-order PDE model. If the noisy image has too many small textures, we may choose the MCD model, because the MCD model may keep small texture better. At last, our model may find a balanced result between the texture and the structure of the image with the change of λ according to the actual need. In many cases, our model performs better than the MCD model in some texture image, because it is hard to define the quantity of texture in the noisy image in actual application. In the later part of this section, we will give the effects of our model with the change of λ.

TABLE VI: MSE and PSNR analysis with the variation of λ

Methods	MSE	PSNR
0	2909.7	22.3474
0.1	517.5	125.6481
0.2	266.2	244.2254
0.3	239.9	271.0192
0.4	253.5	256.4809
0.5	275.0	236.4534
0.6	300.1	216.6842
0.7	325.1	199.9994
0.8	349.2	186.2068
0.9	370.5	175.5235
1.0	391.9	165.9341

Figure 6 shows the effect of our model on Bag image with $\lambda = 0.2, 0.4, 0.6, 0.8$. With the increasing of λ from 0 to 1, we find our model losing more and more texture. We see from figure 6 that the noisy bag image is more and more smooth when λ increase. Meanwhile, the feature of details of the image becomes more and more vague with the change of λ. We also give the MSE and PSNR of the Bag image when λ changes from 0 to 1 with step-size=0.1. We find our model on Bag image will have better denoising effect with λ nearly at interval (0.2 , 0.6).

IV. Conclusion

In this paper, a new model based on the fourth-order PDE and the mean curvature for image restoration is proposed. Due to the choice of λ, our model may not have more broad adaptability than other adaptive smoothing methods, such as the methods proposed in [10, 5] in some cases. But the new model performs better on textured images with appropriate choice of λ. It can preserve the texture better with a distinct effect of denoising. We also give some theoretical analysis of the new model. Based on the numerical experiment, near-perfect theoretical agreement with experiment was achieved.

Acknowledgment

This work is supported by Natural Science Foundation of Jiangxi Province under Grant No. 2010GZS0010, and Project of Education Office of Jiangxi Province.

References

[1] Yu-Li You and M. Kaveh. *Fourth-order partial differential equations for noise removal*. IEEE Transactions on Image Processing, vol. 9, Oct. 2000, pp. 1723-1730,.

[2] Adel I. El-Fallah and Gary E. Ford. *Mean curvature evolution and surface area scaling in image filtering*. IEEE Transactions on Image Processing, vol. 6, No.5, May 1997.

[3] Anthony Yezzi, *Modified Curvature Motion for Image Smoothing and Enhancement*. IEEE TRANSACTIONS ON IMAGE PROCESSING, VOL. 7, NO. 3, MARCH 1998: 345-352.

[4] B. Romeny, ed., *Geometry Driven Diffusion in Computer Vision*. Kluwer, 1994.

[5] S. Kim, H. Lim, *Fourth-order partial differential equations for effective image denoising*. Electronic Journal of Differential Equations, Conf. 17(2009), pp. 107-121.

[6] D Yi, S Lee. *Fourth-order partial differential equations for image enhancement*. Applied Mathematics and Computation,vol. 175, pp. 430-440, April 2006.

[7] M. Lysaker, A. Lundrvold, and X.-C. Tai. *Noise removal using fourth-order partial differential equation with applications to medical magnetic resonance images in space and time*. IEEE Trans. Image Process., vol. 12, no. 12, pp. 1579-1590, 2003

[8] T Chan, J Shen. *Mathematical models for local non-texture inpainting*. SIAM Journal of Application Mathematics, vol. 62, pp. 1019-1043, September 2001.

[9] T. Chan, S. Osher, and J. Shen. *The digital TV filter and nonlinear denoising*. Department of Mathematics, University of California, Los Angeles, CA 90095-1555, Technical Report #99-34, October 1999.

[10] L. Rudin, S. Osher, and E. Fatemi. *Nonlinear total variation based noise removal algorithms*. Physica D, vol. 60, pp. 259-268, 1992.

[11] L. Alvarez, P. Lions, and M. Morel. *Image selective smoothing and edge detection by nonlinear diffusion*. II, SIAM J. Numer. Anal., vol 29, pp.845-866, 1992.

[12] S H Lee, J K Seo. *Noise removal with Gauss curvature-driven diffusion*. IEEE Transactions on Image Processing, vol. 14, pp. 904-909, July 2005.